ELSEVIER

Inorganica Chimica Acta 284 (1999) 229–236

Inorganica Chimica Acta

Ligand substitution kinetics in $M(CO)_4$ ($\eta^{2:2}$-1,5-cyclooctadiene) complexes (M=Cr, Mo, W) — substitution of 1,5-cyclooctadiene by bis(diphenylphosphino)alkanes

Ceyhan Kayran[a], Ferda Kozanoglu[a], Saim Özkar[a,*], Saltuk Saldamlı[a], Aysin Tekkaya[a], Cornelius G. Kreiter[b]

[a] *Department of Chemistry, Middle East Technical University, 06531 Ankara, Turkey*

[b] *Fachbereich Chemie, Universität Kaiserslautern, Erwin-Schrödinger-Strasse, D-67663 Kaiserslautern, Germany*

Received 12 March 1998; accepted 1 July 1998

Abstract

The thermal substitution kinetics of 1,5-cyclooctadiene (COD) by bis(diphenylphosphino)alkanes (PP), $(C_6H_5)_2P(CH_2)_nP(C_6H_5)_2$ ($n = 1$, 2, 3) in $M(CO)_4(\eta^{2:2}$-COD) complexes (M = Cr, Mo, W), were studied by quantitative FT-IR spectroscopy. The reaction rate exhibits first-order dependence on the concentration of the starting complex, and the observed rate constant depends on the concentration of the leaving COD ligand and on the concentration and the nature of the entering PP ligand. In the proposed mechanism, the rate determining step is the cleavage of one metal–olefin bond of the COD ligand. A rate-law is derived from the proposed mechanism. The evaluation of the kinetic data gives the activation parameters which support an associative mechanism in the transition states. Both the observed rate constant and the activation parameters show little variation with the chain length of the diphosphine ligand.

Keywords: Ligand substitution; Molybdenum complexes; Tungsten complexes; Diphosphine complexes; Kinetics and mechanism

1. Introduction

In a recent paper [1] we reported on the kinetics of the thermal substitution of 1,5-cyclooctadiene from $[Mo(CO)_4(\eta^{2:2}$-COD] (by bis(diphenylphosphino)methane (DPPM) as a model reaction for the displacement of a formally bidentate diene ligand in the octahedral coordination sphere of a low valent metal by a bidentate donor ligand. It was found that the weakly bound COD ligand is replaced by DPPM at an observable rate in the temperature range of 35–50°C to form the known complex $[Mo(CO)_4$(DPPM] as the final product [2,3]. The kinetics of this thermal substitution reaction were studied by quantitative FT-IR spectroscopy. The reaction rate exhibits first-order dependence on the concentration of $[Mo(CO)_4(\eta^{2:2}$-COD)], and the observed rate constant depends on the concentrations of both leaving COD and entering DPPM ligands. A rate law was derived from the proposed mechanism in which the rate determining step is the cleavage of one of two Mo–olefin bonds. Here, we report about our extended study on the displacement kinetics of COD from $M(CO)_4(\eta^{2:2}$-COD) (M = Cr (**1A**), Mo (**2A**), W (**3A**)) by bis(diphenylphosphino)alkanes (PP), $(C_6H_5)_2P(CH_2)_nP(C_6H_5)_2$ ($n = 1$ (**B**), 2 (**C**), 3 (**D**)) with the aim to investigate the dependence of the reaction kinetics on the nature of the metal and on the chain-lengths of the PP ligands.

$$\underset{\mathbf{1A-3A}}{M(CO)_4(\eta^{2:2}\text{-COD})} + \underset{\mathbf{B-D}}{PP} \xrightarrow{\Delta} \underset{\mathbf{1B-3D}}{M(CO)_4(PP)} + COD$$

where M = Cr, Mo, W; $PP = (C_6H_5)_2P(CH_2)_nP(C_6H_5)_2$; $n = 1, 2, 3$

The quantitative FT-IR spectroscopy was used to study the kinetics of these ligand displacement reactions. Monitoring the intensities of the absorption bands of the CO stretching vibrations for both the reactant and the product enables one to determine the changes in their concentrations, thus to follow the reaction precisely, and to check the material balance and the yield throughout the reaction.

*Corresponding author. Tel.: +90-312-210-1280; fax: +90-312-210-3212.

0020-1693/99/$ – see front matter
PII: S0020-1693(98)00293-X

2. Experimental

All reactions and manipulations were carried out either in vacuo or under a dry and oxygen-free nitrogen atmosphere. Solvents were distilled after refluxing over metallic sodium or phosphorous pentoxide for 3–4 days and stored under nitrogen until used. Hexacarbonylchromium(0), hexacarbonylmolybdenum(0), hexacarbonyltungsten(0), 1,5-cyclooctadiene (**A**), bis(diphenylphosphino)methane (**B**), 1,2-bis(diphenylphosphino)ethane (**C**), and 1,3-bis(diphenylphosphino)propane (**D**) were purchased from Aldrich Chemical, England. The thermal reactions and other treatments of organometallic compounds such as purification and crystallisation were followed by taking IR spectra at appropriate time intervals. NMR spectra were recorded on a Bruker AC-200 spectrometer (200.131 MHz for ^{1}H, 81.011 MHz for ^{31}P, and 50.28 MHz for ^{13}C). TMS was used as internal reference for ^{1}H and ^{13}C NMR chemical shifts. Phosphoric acid (85%) in a capillary tube was used as external reference for ^{31}P NMR chemical shifts. Infrared spectra were recorded from solutions on a Perkin-Elmer 16 PC FT-IR spectrometer. Photochemical reactions were carried out in an immersion-well apparatus [4] (solidex glass, >280 nm) using a Hanau TQ 150 high pressure mercury lamp, which was cooled by circulating water or cold methanol. A circulating thermostat bath (Heto CB 11e) was used to provide a constant temperature during the kinetic measurements. Ethylene glycol was circulated from the thermostat through the heating jacket of the reaction vessel.

2.1. Tetracarbonyl($\eta^{2:2}$-1,5-cyclooctadiene)metal(0)

Tetracarbonyl($\eta^{2:2}$-1,5-cyclooctadiene)-chromium(0), $Cr(CO)_4(\eta^{2:2}$-COD) (**1A**), and tetracarbonyl($\eta^{2:2}$-1,5-cyclooctadiene)tungsten(0), $W(CO)_4(\eta^{2:2}$-COD) (**3A**), were prepared by irradiation of hexacarbonylmetal(0) and COD in *n*-hexane at room temperature using a procedure described in literature [5]. When all hexacarbonylmetal(0) was consumed, due to IR monitoring, the mixture was filtered to remove colloidal decomposition products. The excess solvent and COD were removed under reduced pressure. The residue was dissolved in *n*-hexane and the solution was allowed to stand for 1 day at −35°C for crystallisation. The solvent was decanted and crystals were dried in vacuo. Tetracarbonyl($\eta^{2:2}$-1,5-cyclooctadiene)-molybdenum(0), $Mo(CO)_4(\eta^{2:2}$-COD) (**1B**), was prepared by refluxing a solution of $Mo(CO)_6$ and COD in *n*-heptane for 24 h as described in the literature [1,6]. The solution was worked up in the same way as for the homologous chromium and tungsten complexes.

2.2. Tetracarbonyl-bis(diphenylphosphino)alkane-metal(0)

Equimolar amounts (ca. 1 mol) of $M(CO)_4(\eta^{2:2}$-COD) (**1A–3A**) and $PP = Ph_2P(CH_2)_nPPh_2$ ($n = 1, 2, 3$) (**B–D**) were dissolved in toluene (50 ml) and refluxed for several minutes. Cooling the solution to −35°C yields pale yellow crystals of $M(CO)_4$(PP) (**1B–3D**) which are separated from the supernatant liquid by decantation and dried under vacuum and identified by ^{13}C and ^{31}P NMR spectroscopy [7].

2.3. Kinetic measurements

All kinetic measurements were conducted on toluene solutions in a Specac variable temperature IR cell with a 0.129 mm path length and calcium fluoride windows. Extinction coefficients of $M(CO)_4(\eta^{2:2}$-COD) (**1A–3A**) and $M(CO)_4$(PP) (**1B–3D**) were determined from toluene solutions of the pure complexes by plotting the absorbance of the ν(CO) IR band with the highest frequency versus the concentration of the respective complex in the range of 5×10^{-4} to 1×10^{-2} mol l^{-1} (Table 1). Using these values, the concentrations of the complexes during the reactions of **1A–3A** with PP could be determined from the measured IR absorbances at any stage of the reactions. Thus the material balance could also be checked at any point of conversion.

Table 1
The CO stretching frequencies (cm^{-1}) for the complexes and molar extinction coefficient (mol l^{-1} cm^{-1}) for the highest frequency band in toluene

Complex	ε for $A_{1(2)}$	$A_{1(2)}$	$A_{1(1)}$	B_1	B_2
$Cr(CO)_4(\eta^{2:2}$-COD) (**1A**)	2515	2023	1927	1942	1893
$Mo(CO)_4(\eta^{2:2}$-COD) (**2A**)	2514	2035		1940	1890
$W(CO)_4(\eta^{2:2}$-COD) (**3A**)	2602	2035		1941	1888
$Cr(CO)_4$(DPPM) (**1B**)	3301	2012	1922	1903	1891
$Mo(CO)_4$(DPPM) (**2B**)	3520	2012	1930	1901	1890
$W(CO)_4$(DPPM) (**3B**)	4526	2012	1923	1902	1889
$Cr(CO)_4$(DPPE) (**1C**)	2983	2020	1929	1917	1897
$Mo(CO)_4$(DPPE) (**2C**)	3119	2017	1928	1908	1897
$W(CO)_4$(DPPE) (**3C**)	1316	2023	1936	1908	
$Cr(CO)_4$(DPPP) (**1D**)	4534	2015	1935	1907	1890
$Mo(CO)_4$(DPPP) (**2D**)	4215	2015	1930		1883
$W(CO)_4$(DPPP) (**3D**)	1910	2016	1933	1901	1888

The $M(CO)_4(\eta^{2:2}$-COD) complexes were added into the solutions of the diphosphane in toluene at low temperature to avoid any reaction. The initial concentration (C_o) of the complexes was around $= 0.01$ mol l^{-1}. A sample of this solution was put into the IR cell preheated to the reaction temperature. The IR spectra were recorded periodically as the reaction proceeded at constant temperature. The rates of the reaction were determined by following the disappearance of the highest frequency ν(CO) band of the educt since it was the only distinct band which does not overlap with the bands of the products. By this way, quantitative data on the rates of reactions were collected easily and accurately. The graphical evaluation of the data provides the observed rate constants. In order to study the dependence of the rate on the leaving COD and entering PP, the kinetic experiments were performed by varying the concentrations of PP (0.01–0.50 mol l^{-1}) or COD (0.0–0.1 mol l^{-1}) in the solutions of **1A–3A** ($C_o = 0.01$ mol l^{-1}) at 40 (M = Cr), 45 (M = Mo), and 90°C (M = W). The activation parameters were determined from the temperature dependence of the observed rate constant in the range of 40–90°C.

3. Results and discussion

The IR absorption spectra of both $M(CO)_4(\eta^{2:2}$-COD) and $M(CO)_4$(PP) complexes taken in toluene show four absorption bands in the CO stretching region indicating a *cis* arrangement of four CO groups in the pseudo-octahedral coordination sphere of the metal (Table 1). Thus the $M(CO)_4$ unit in the complexes has a local C_{2v} symmetry with two $A_1+B_1+B_2$ CO stretching modes [8]. Complexes **2A**, **3A**, **3B**, and **2D** give only three IR–CO stretching bands indicating that two of the four expected bands are accidentally degenerated.

The kinetics of the thermal substitution of COD from **1A–3A** by bis(diphenylphosphino)alkanes were followed using the quantitative FT-IR spectroscopy. In the ν(CO) region of the IR spectrum, the absorption bands of **1A–3A** are gradually replaced by the new bands of the corresponding product $M(CO)_4$(PP) in the course of the displacement reaction. The gradual change in the IR spectrum during the reaction of $W(CO)_4(\eta^{2:2}$-COD) (**3A**) with DPPM (**B**) at 90°C, as an example, is depicted in Fig. 1. The observation of nice isosbestic points indicates a straightforward conversion of the reactant into the product without side or subsequent reactions [9]. In other words there are only two absorbing species throughout the reaction. Another point emerging from the inspection of the IR spectra at first glance is that the highest frequency bands of the reactant and the product do not overlap and remain well resolved during the whole reaction. Therefore, these two IR bands are selected to follow the consumption of the educt and the growth of the product, respectively.

Fig. 2(a) shows the time-dependent behaviour of concentrations of the reactant and the product in the course of the thermal substitution reaction of **3A** with **B** in toluene at 90°C, for which the time-resolved IR spectra are given in Fig. 1. This graph shows an exponential decay for the starting complex **3A** and an exponential growth for the product **3B**. The logarithmic plot of the concentration of the reactant against time gives a straight line (Fig. 2(b)) for the aforementioned reaction even at low concentrations of bis(diphenylphosphino)methane. This indicates that the displacement of COD from **1A–3A** by PP obeys the pseudo-first-order kinetics with a correlation constant greater than 0.99. The slope of the straight line gives the observed rate constant, k_{obs} (s^{-1}), for the pseudo-first-order thermal substitution reaction.

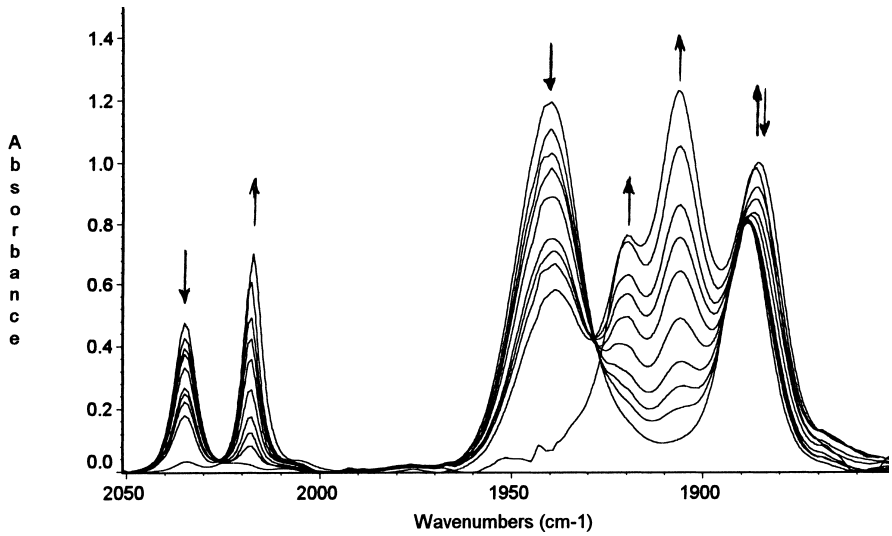

Fig. 1. The gradual change in the IR spectrum during the thermal substitution reaction of COD from $W(CO)_4(\eta^{2:2}$-COD) (**3A**), by DPPM to yield $W(CO)_4$(DPPM) (**3B**), at 90°C in toluene.

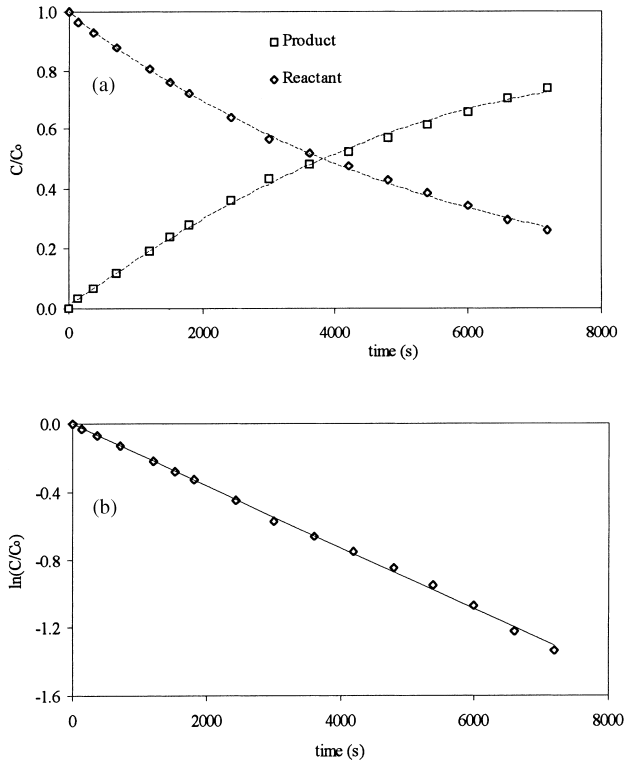

Fig. 2. Time dependent behaviour of concentrations of the reactant and product during the thermal substitution reaction of COD from $W(CO)_4(\eta^{2:2}$-COD) (**3A**) by DPPM at 90°C. (a) Concentration versus time plot for $W(CO)_4(\eta^{2:2}$-COD) (**3A**) and $W(CO)_4(\eta^{2:2}$-DPPM) (**3B**), (b) plot of the first-order reaction kinetics for the consumption of $W(CO)_4(\eta^{2:2}$-COD) (**3A**).

The kinetic data for the COD substitution in $M(CO)_4(\eta^{2:2}$-COD) by the diphosphinoalkanes are consistent with the mechanism (Scheme 1) proposed for the same substitution in the homologous molybdenum complex by DPPM [1]. The reaction involves a stepwise displacement of COD from $M(CO)_4(\eta^{2:2}$-COD) by PP. The initial rate determining step is the cleavage of one of the metal–diene bonds [10].

A series of experiments were performed to check whether a CO detachment would occur as an initial step. First of all, none of the three starting complexes **1A–3A** gives any reaction in the absence of entering ligand upon heating to the temperature at which the ligand substitution takes place at appreciable rate. In a similar reaction under 1 atm CO at the same temperature the starting complex is completely converted into the corresponding hexacarbonylmetal(0) within 2 to 4 h. Heating solutions of the starting complexes **1A–3A** in the presence of equimolar amounts of PP under a CO atmosphere at the same temperature give rise to the formation of $M(CO)_4$(PP) predominantly, and $M(CO)_5$(PP) and $M(CO)_6$ in low concentrations (less than 15 or 5%, respectively). Working in the presence of a 10-fold excess of PP, $M(CO)_4$(PP) is solely obtained as product.

All these results, in particular the formation of $M(CO)_5$(PP), indicate that the initial step is the cleavage of one metal–olefin bond forming the $M(CO)_4(\eta^2$-COD) intermediate **I**, and not the CO detachment (Scheme 1). The intermediate **I** can either return to the starting complexes **1A–3A** by a recomplexation step of the free CC double bond or go on to the next steps. Competition between the associative and dissociative processes involving the leaving and entering ligands will determine the subsequent steps. Intermediate **I** can undergo an associative reaction with COD or PP leading to the formation of intermediates **III** and **IV**, respectively, whereby COD and PP are coordinated to the

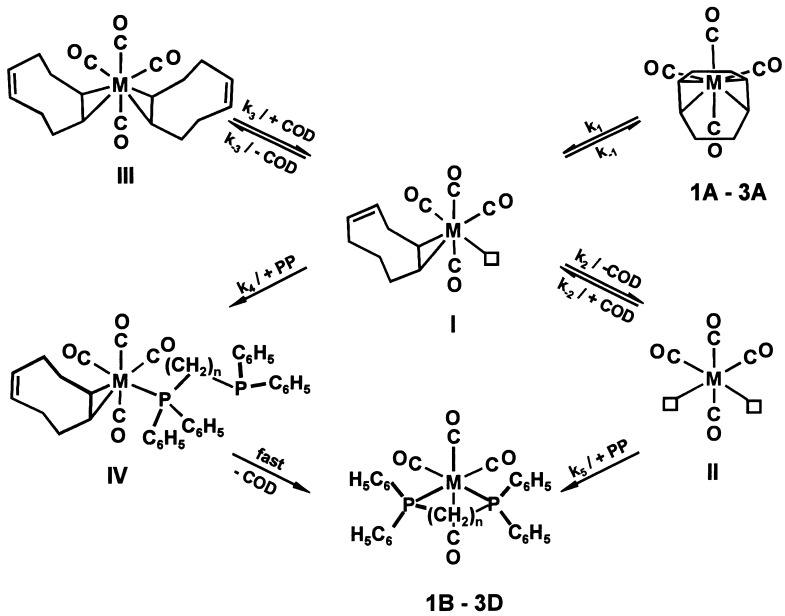

Scheme 1. Mechanism proposed for the substitution of COD from $M(CO)_4(\eta^{2:2}$-COD) by bis(diphenylphosphino)alkane (PP).

transition metal in a monodentate fashion. A complete cleavage of COD from the intermediate **I** has also to be considered, leading to the unstable 14-electron intermediate $M(CO)_4$ (**II**), which will react immediately with PP to form the final products **1B–3D**. On the other hand, when COD is cleaved from intermediate **IV** the rapid chelation of PP also yields **1B–3D**. This mechanism differs from the one proposed for the same type of reaction with the two-term rate law [11,12], which does not consider the recoordination of COD to the unstable 14-electron intermediate $M(CO)_4$ (**II**) and, therefore, can not explain the dependence of the observed rate constant on the COD concentration. The mechanism proposed here also considers this point.

The rate law of the thermal ligand substitution reaction can be obtained from the proposed mechanism (Scheme 1) by applying the well-known steady state approximation for the intermediates **I**, **II**, and **III**.

$$\text{rate} = k_{obs}[M(CO)_4(\eta^{2:2}\text{-COD})] \quad (2)$$

$$k_{obs} = k_1 - \frac{k_1 k_{-1}}{k_{-1} + k_2 + k_4[PP] - k_2/(1 + k_5[PP]/k_{-2}[COD])} \quad (3)$$

The rate of the reaction shows first-order dependence on the concentration of $M(CO)_4(\eta^{2:2}$-COD) and the observed rate constant, k_{obs}, depends on the concentration of COD and PP. Of course, Eq. (3) could be simplified by using some assumptions. However, such assumptions would be valid only under specific conditions. Below we will show that the proposed mechanism is in agreement with the experimental results in general (Table 2).

First of all, the observed rate constant is found to increase with the increasing concentration of PP. For the thermal substitution of COD from **1A** by **B**, the observed rate constant is plotted versus the concentration of **B** as an illustrative example (Fig. 3). No noticeable change is observed for the concentration of $M(CO)_4(\eta^{2:2}$-COD) when the reaction is carried out in the absence of PP at temperatures at which ligand substitution takes place normally at an appreciable rate. This clearly indicates that the observed rate constant is zero in the absence of PP, as predicted by the proposed mechanism. The limit of k_{obs} approaches zero, when the concentration of **B** goes to zero.

$$\lim_{[PP]\to 0} k_{obs} = 0 \quad (4)$$

As the concentration of the entering ligand increases gradually, the observed rate constant increases and reaches a saturation limit at a high concentration of PP.

$$\lim_{[PP]\to\infty} k_{obs} = k_1 \quad (5)$$

The first limiting value of the observed rate constant is zero for all three $M(CO)_4(\eta^{2:2}$-COD) complexes while the second limiting value, k_1, depends on the central metal in the starting complexes. The values of k_1 are 1.09×10^{-3} s^{-1} for M = Cr at 313 K, 2.0×10^{-3} s^{-1} for M = Mo at 318 K, and 2.4×10^{-4} s^{-1} for M = W at 363 K. The k_1 value for $Mo(CO)_4(\eta^{2:2}$-COD) is consistent with the value of $0.2 \times 10^{4-}$ s^{-1} reported for the same complex at 303 K [11,12]. Although it is not possible to make a meaningful comparison of the k_1 values for the three complexes at different temperatures, the COD ligand in **3A** seems to be much less labile than that in the complexes **1A** and **2A**.

Increasing concentrations of COD cause a decrease in the observed rate constant as illustrated in Fig. 4. The plot of the observed rate constant versus the concentration of COD for the COD substitution in **1A–3A** by **B** is curved downward, starting with a positive intercept.

$$\lim_{[COD]\to 0} k_{obs} = k_1 - \frac{k_1 k_{-1}}{k_{-1} + k_2 + k_4[PP]} \quad (6)$$

As the concentration of COD goes to zero, the limiting value

Table 2
The relationships between the individual rate constants in the COD substitution reactions of **1A–3A** by DPPM

1A at 313 K	**2A** at 318 K	**3A** at 363 K
$k_{-1} = 5.9\ k_4[PP]$	$k_{-1} = 11.4\ k_4[PP]$	$k_{-1} = 11.8\ k_4[PP]$
$k_{-1} = 9.7\ k_2$	$k_{-1} = 23.3\ k_2$	$k_{-1} = 14.8\ k_2$
$k_4[PP] = 1.7\ k_2$	$k_4[PP] = 2.04\ k_2$	$k_4[PP] = 1.25\ k_2$

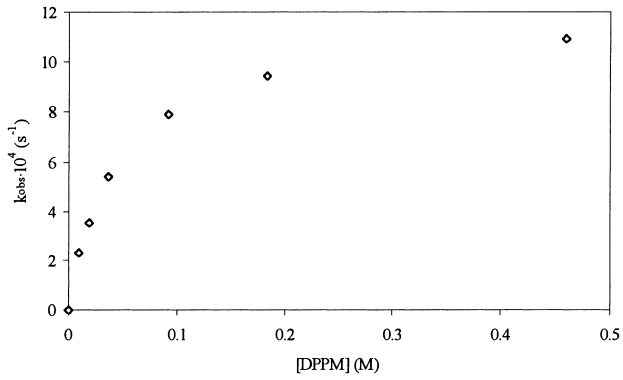

Fig. 3. Variation of the observed rate constant with the concentration of the entering ligand for the thermal substitution reaction of COD from $Cr(CO))_4(\eta^{2:2}$-COD) (**1A**) by DPPM at 40°C.

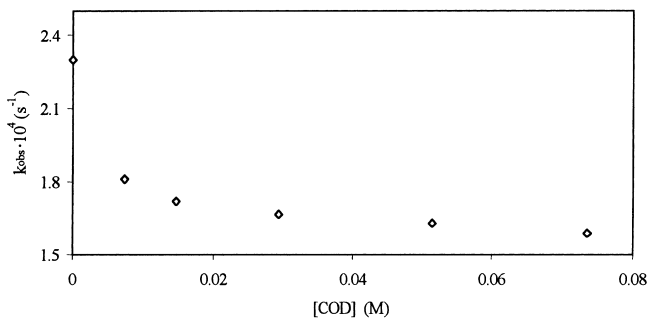

Fig. 4. Variation of the observed rate constant with the concentration of COD for the thermal substitution reaction of COD from $Cr(CO)_4(\eta^{2:2}$-COD) (**1A**) by DPPM in one-fold concentration at 40°C.

of k_{obs} for the COD substitution in **1A–3A** is found to be 2.3×10^{-4}, 2.3×10^{-4}, and 4.6×10^{-5} s^{-1} at 313, 318, and 363 K, respectively. The observed rate constant decreases with increasing concentration of COD, reaching another saturation limit at high concentrations.

$$\lim_{[COD]\to\infty} k_{obs} = k_1 - \frac{k_1 k_{-1}}{k_{-1} + k_4[PP]} \quad (7)$$

The saturation limits of k_{obs} for the COD substitution in **1A–3A** are found to be 1.6×10^{-4}, 1.6×10^{-4}, and 1.9×10^{-5} s^{-1} at temperatures given above. The decrease in k_{obs} caused by the increasing concentration of COD clearly suggests that the substitution rate of COD in the starting complex is slowed down in the presence of excess COD in the solution. In other words, the starting complex is stabilised by the presence of excess COD. All these findings are consistent with the proposed mechanism (Scheme 1). From the four limiting values of the observed rate constant, one can obtain some useful relationships between the individual rate constants in the substitution reactions for the three metals (Table 2). Two important points emerge from the comparison of the relationships in Table 2. The first one is that k_{-1} is much greater than both k_2 and k_4[PP] for all the three COD complexes, being attributed to the chelate effect [13]. The second point is that the values of k_4[PP] and k_2 are almost comparable. The change in the k_4[PP]/k_2 ratio on going from chromium through tungsten cannot be interpreted in a simple manner because the reaction temperatures for the respective complexes are different. An increase in this ratio on going from chromium through tungsten would be expected from the competition between the associative and dissociative reactions of **I** to form the intermediates **II** and **IV**, respectively. On passing from chromium to the larger molybdenum or tungsten, the associative pathway would be becoming dominant. However, the increased temperatures may favour the dissociative term k_2.

The ligand substitution reaction of **2A** was performed using three different diphosphines (**B–D**), in order to investigate the dependence of the observed rate constant on the chain length. A plot of k_{obs} versus PP gives curves for the three diphosphine ligands, which are barely different from each other. For a better appreciation of this dependence, the values of $1/(k_1 - k_{obs})$ instead of k_{obs} (Eq. (8)) are plotted against the concentration of PP (Fig. 5).

$$\frac{1}{k_1 - k_{obs}} = \frac{1}{k_1 k_{-1}} \times \left[k_{-1} + k_2 + k_4[PP] - \frac{k_2}{(1 + k_5[PP]/k_{-2}[COD])} \right] \quad (8)$$

All of the three PPs show the same effect up to a concentration of 0.1 mol l^{-1} which corresponds to a 10-fold excess of PP relative to the starting complexes; the value of $1/(k_1 - k_{obs})$, thus k_{obs}, increases slightly with the increasing concentration of PP. At higher concentrations of PP, however, the observed rate constant shows strong dependence on the concentration and the nature of the entering ligand. This observation indicates that the last term in the expression for $1/(k_1 - _{obs})$ (Eq. (8)) is negligible at high concentrations of PP. The order observed for the $1/(k_1 - k_{obs})$ value (DPPM<DPPE<DPPP) at high concentrations is consistent with the basicity of the chelating PPs [14].

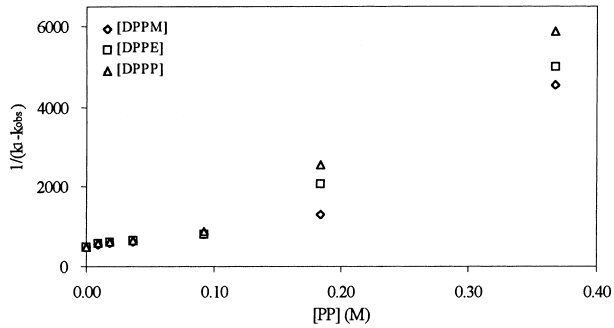

Fig. 5. Dependence of the observed rate constant on the nature and concentration of the diphosphine ligand for the thermal ligand substitution of $Mo(CO)_4(\eta^{2:2}$-COD) (**2A**) at 45°C.

The substitution kinetics of COD in **2A** were studied for all of the three PPs at different temperatures in the presence of a 10-fold excess of PP to ensure the pseudo-first-order condition. The Eyring plots for the thermal ligand substitution are given in Fig. 6 for the three PPs which give straight lines. The activation parameters obtained from the evaluation of the Eyring plots in Fig. 6 are $\Delta H^{\neq} = 80 \pm 1, 85 \pm 1, 69 \pm 1$ kJ mol^{-1}, and $-\Delta S^{\neq} = 55 \pm 2, 38 \pm 2, 86 \pm 2$ J K^{-1} mol^{-1}, respectively. Although the mechanism proposed for the COD substitution in **2A** is expected to be valid for all of the three PPs, some variations are noticeable in both the enthalpy and entropy of activation. A plot of $\Delta H^{\neq}$ versus $\Delta S^{\neq}$ allows a better interpretation of the enthalpy and entropy values [15,16]. The observation of a straight line for the $\Delta H^{\neq} - \Delta S^{\neq}$ plot indicates that the COD substitution in **2A** follows a common mechanism for all of the three entering ligands. The isokinetic temperature [17,18] of 326 K is obtained from the slope of the $\Delta H^{\neq} - \Delta S^{\neq}$ line. Although the observed rate constants depend upon the nature and concentration of the entering ligand, the activation enthalpy and entropy of the ligand substitution reaction is found to follow the same mechanism independent of the entering PP. This may be attributed to the fact that the PP ligands form metal–phosphorus bonds of similar strengths independent of the chain length.

The material balance does not show a significant depletion up to 80–90% conversion for all of the thermal ligand substitution reactions studied. This could be due to the fact that the diphosphines form stable $M(CO)_4$(PP) complexes. Therefore, the presence of excess PP or COD in the reaction solution does not affect the material balance and the yield of $M(CO)_4$(PP) formed in each set of experiments.

The substitution kinetics of COD in $M(CO)_4(\eta^{2:2}$-COD) by DPPM were studied for all of the three complexes at different temperatures in the presence of a 50-fold excess of

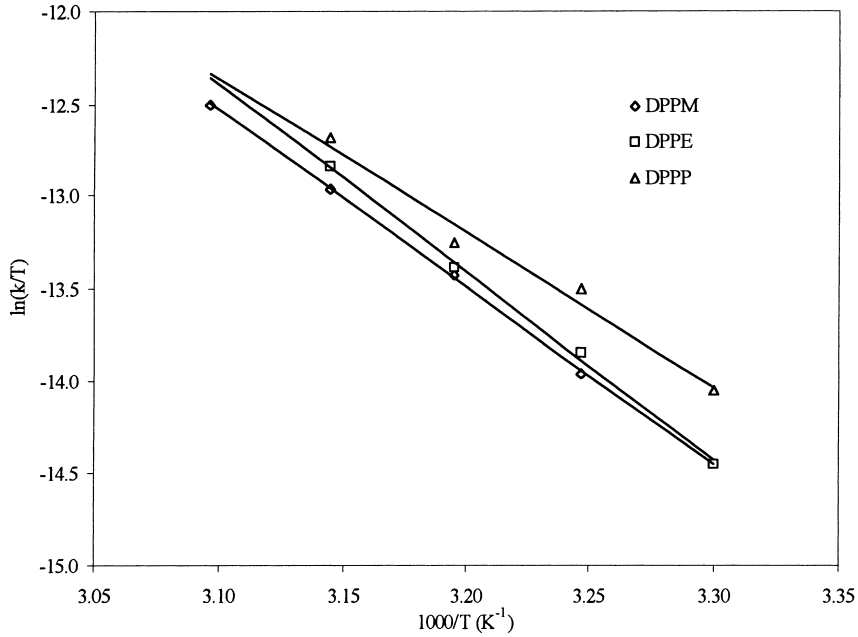

Fig. 6. Eyring plot for the substitution of COD in $Mo(CO)_4(\eta^{2:2}$-COD) (**2A**) by diphosphine (DPPM, DPPE, and DPPP) in a 10-fold excess.

PP to ensure the pseudo-first-order condition. The values obtained for the observed rate constants at four different temperatures practically correspond to k_1 for the respective complexes. However, the values of the observed rate constants can be used to estimate the activation enthalpy and entropy values for the overall reaction by drawing the Eyring plots as the contribution of all the other steps may be still significant under the experimental conditions. The values found are $\Delta H^{\neq} = 82 \pm 1$, 79 ± 2, 89 ± 3 kJ mol^{-1}, and $\Delta S^{\neq} = -41 \pm 3$, -53 ± 5, -79 ± 6 J K^{-1} mol^{-1}, for M = Cr, Mo, W, respectively. The large negative value of the activation entropy for all the complexes is indicative of an associative mechanism in the transition states [19,20]. If some associated species were a reactive form of the complexes, an equilibrium between the complex and this species would result in a ligand dependence of the rate constants at low ligand concentrations [21]. In other words, the dependence of the reaction rate on the ligand concentrations can easily be explained by a displacement mechanism which proceeds via the formation of seven-coordinated complexes in the transition states [22,23]. Although this is unusual for octahedral complexes, they may undergo substitution reactions by an associative mechanism [24]. Support for this assignment of an associated mechanism in the transition states for the COD displacement reactions of chromium, molybdenum and tungsten complexes comes from the comparison of the activation enthalpies with the metal–olefin bond energies. The rate-determining step involves only a metal–olefin bond breaking in the dissociative S_N1 mechanism and a total metal-COD cleavage and bond making (M–PP) in the associative S_N2 mechanism [24]. The activation enthalpy is therefore expected to approach the metal–olefin bond energy for a predominantly dissociative mechanism, whereas for an associative process $\Delta H^{\neq}$ is expected to be rather smaller than the metal–olefin bond energy [25]. The activation enthalpies for the displacement of COD from the $M(CO)_4(\eta^{2:2}$-COD) complexes are smaller than the corresponding metal–olefin bond energies (e.g. 108 kJ mol^{-1} for molybdenum–COD) [26].

Acknowledgements

Support of this work by Volkswagen Stiftung and TÜBITAK under Grant No. TBAG-1226 is gratefully acknowledged.

References

[1] A. Tekkaya, C. Kayran, S. Özkar, C.G. Kreiter, Inorg. Chem. 33 (1994) 2439–2443.
[2] J. Chatt, H.R. Watson, J. Chem. Soc. (1961) 4980–4988.
[3] K.K. Cheung, T.F. Lai, K.S. Mok, J. Chem. Soc. (A) (1971) 1644–1647.
[4] F.-W. Grevels, J.G.A. Reuvers, J. Takats, Inorg. Synth. 24 (1986) 176–180.
[5] M. Kotzian, C.G. Kreiter, S. Özkar, J. Organomet. Chem. 229 (1982) 29–42.
[6] E.O. Fischer, W. Fröhlich, Chem. Ber. 92 (1959) 2995–2998.
[7] G.T. Andrews, I.J. Colquhoun, W. McFarlane, Polyhedron (1983) 783–790.
[8] P.S. Braterman, Metal Carbonyl Spectra, Academic Press, London, 1975.
[9] B.S. Creaven, F.-W. Grevels, C. Long, Inorg. Chem. 28 (1989) 2231–2234.
[10] D.T. Dixon, P.M. Burkinshaw, J.A.S. Howell, J. Chem. Soc., Dalton Trans. (1980) 2237–2240.

[11] F. Zingales, M. Graziani, U. Belluco, J. Am. Chem. Soc. 89 (1967) 256–260.
[12] F. Zingales, F. Canziani, F. Basolo, J. Organomet. Chem. 7 (1967) 461–471.
[13] F. Basolo, R.G. Pearson, Mechanisms of Inorganic Reactions, 2nd ed., Wiley, New York, 1958.
[14] J.R. Sowa, R.J. Angelici, Inorg. Chem. 30 (1991) 3534–3537.
[15] J.E. Leffler, J. Org. Chem. 20 (1995) 1202–1231.
[16] J.E. Leffler, J. Org. Chem. 31 (1966) 533–537.
[17] W. Linert, Chem. Soc. Rev. 18 (1989) 477–505.
[18] W. Linert, Chem. Soc. Rev. 23 (1994) 429–438.
[19] R.G. Wilkins, Kinetics and Mechanism of Reactions of Transition Metal Complexes, 2nd ed., VCH, Weinheim, 1991.
[20] R.J. Angelici, J.R. Graham, J. Am. Chem. Soc. 87 (1965) 5586–5590.
[21] J.R. Graham, R.J. Angelici, J. Am. Chem. Soc. 87 (1965) 5590–5597.
[22] R.J. Angelici, J.R. Graham, J. Am. Chem. Soc. 88 (1966) 3658–3659.
[23] J.R. Graham, R.J. Angelici, Inorg. Chem. 6 (1967) 2082–2085.
[24] R.G. Pearson, D.N. Edgington, F. Basolo, J. Am. Chem. Soc. 84 (1962) 3233–3237.
[25] J.A. Connor, J.P. Day, E.M. Jones, G.K. McEwen, J. Chem. Soc., Dalton Trans. (1973) 347–354.
[26] S.L. Mukerjee, S.P. Nolan, C.D. Hoff, R.L. de La Vega, Inorg. Chem. 27 (1988) 81–83.